Investigation of the Tendency for Failure of Refractory Castables in the Wear Lining of a Steel Ladle Using Elongated or Cubic Shaped Tabular Alumina

E. Brochen, M. Sollbach, Chr. Dannert, O. Krause, L. Erbar, S. Abdelouhab, P. Pilate

Over the past decades, numerical simulation has proved to be a decisive tool for engineers. In the field of refractory technologies, numerical modelling helps increasing the understanding of the behaviour of refractory linings under service conditions, checking the validity of new designs and potentially predicting the failure of refractory structures. However, due to the arising of complex states of stresses during operation, the prediction of the failure of complex refractory structures, such as linings, is no easy task. On the one hand, refractory materials, like most ceramic materials, tend to be weak in tension but strong in compression. On the other hand, very complex stress distributions are generated in refractory structures under operation. Consequently, no simple and single strength thresholds, such as the tensile or compression strength, can be used in a straightforward and obvious manner. Failure thresholds considering complex multiaxial state of stress need to be implemented.

As one of the pertinent failure criteria for refractory structures, the Drucker-Prager criterion was derived from uniaxial compression and diametral compression tests and applied to an exemplary model. Focus was laid on the investigation of the tendency for failure of a high alumina monolithic wear lining in a steel ladle during its first heating up. Especially, the impact of using either splintered or cubic tabular alumina in the coarse fraction of the monolithic was studied.

First critical stresses seemed to appear already in the middle of the pre-heating of the steel ladle, i.e. above 500 °C. Using splintered tabular alumina enhanced the cohesion of the castable and improved the resistance to failure of the lining in operation.

1 Introduction

Numerical simulation has become a fundamental tool to investigate complex processes/mechanism or to solve problem in a less expensive way. In the case of refractory applications, two major issues need to be taken into account:

- The refractory material properties and behaviour are strongly temperature dependent, especially for refractory castables that experience strong microstructural changes during the first heating. Results from laboratory tests at room temperature cannot be used to simulate the behaviour of refractory structures exposed to high temperature in service.
- Refractory materials display asymmetric failure behaviour, able to sustain much larger compressive stresses than tensile stresses. This means that no single failure criterion (for instance tensile or compressive strength obtained by laboratory tests) can be used to describe and predict the failure of complex refractory linings in operation.

1.1 Numerical simulation

When studying the behaviour of real-world systems, it becomes soon clear that exact analytic solutions are often either too cumbersome or simply do not exist [1]. However, by

Erwan Brochen, Maren Sollbach, Christian Dannert
Forschungsgemeinschaft Feuerfest e. V.
Höhr-Grenzhausen
Germany

Olaf Krause, Laura Erbar
Hochschule Koblenz
Höhr-Grenzhausen
Germany

Sandra Abdelouhab, Pascal Pilate
INISMa Institut Interuniversitaire des Silicates
Mons
Belgium

Corresponding author: *Erwan Brochen*
E-mail: brochen@fg-feuerfest.de

Keywords: numerical simulation, wear lining, Drucker-Prager failure criterion, particle shape

using algorithms for obtaining approximate numerical solutions, complicated problems can be solved. The Finite Element Method (FEM) is a numerical procedure for solving problems of engineering and physics. It is best known for investigations of stability and deformation of solids with a complex geometry. By dividing the investigated object into smaller pieces, i.e. creating a 3D-mesh, many cells and nodes appear in the component. While solving the entire problem domain at once is impossible, solving the problem iteratively at each of the nodes proved to be an efficient strategy. The space between the nodes gets interpolated. The finer the mesh, the closer the result is to reality, but also the more complex is the calculation.

1.2 Modeling of thermal stresses in refractory structures

The FEM modelling and calculation of thermal stresses in refractory structures implies to respect two closely interlinked stages: The modelling of the system (definition of the model geometry, definition of the materials properties, boundary conditions, creation of a suitable mesh and selection of the right physic/study settings) and the solution of the thermal stress problem.

The development of a successful simulation begins with the preparation of the Computer-Aided Design (CAD) model. Typically this entails a sound analysis of the system to be modelled in order to design a simplified geometry (for instance by removing irrelevant details and using symmetry) while keeping the dimensions and processes to be simulated realistic.

As soon as heat is introduced or removed from a system, temperatures vary until equilibrium is achieved. In solid structures, such as refractory linings of furnaces and processing units, the heat transfer occurs predominantly by means of heat conduction and is described by the Fourier's law of heat transfer. Under operating conditions, large and unsteady thermal gradients arise within components of a refractory lining. As the temperature increases/decreases, the volume elements of refractory linings expand/constrict. Such an expansion/contraction generally cannot proceed freely in a continuous body, and thermal stresses are generated [2]. The calculation of the occurring thermal stresses implies therefore to solve a coupled system of three stress differential equations and the Fourier's differential equation. Practically, this means to determine, at first, the temperature distribution in the refractory structure by solving the Fourier's differential equation. Then, to calculate, from the temperature distribution, the ensuing strains and stresses.

1.3 Failure criteria

In terms of material behaviour, failure is usually defined as the loss of load carrying capacity of a material unit. Traditionally, a distinction is drawn between brittle failure (fracture) and ductile failure (yield). Under most practical situations, a given material can be rated as either brittle or ductile. Due to their typical operating conditions, this distinction is not straightforward for refractory materials. Parts of a refractory lining still experiencing relatively low temperatures may undergo brittle failure, while the parts of the lining subjected to high temperatures are prone to a ductile failure. Additionally, the state of stress and the rate at which stresses develop are likely to further affect the failure mode at a given temperature. For the sake of simplicity, the present work focused on the failure criterion for refractory materials as an indication of the initiation of irreversible deformations or broadly speaking damage, regardless of whether it leads to fracture or yield.

Mathematically, failure criteria are expressed as functions in stress or strain space that separate "failed" states from "unfailed" states. The simplest form of failure criteria, which was developed for brittle materials, just considers the maximum stress/strain that a material can sustain while being stretched or compressed before failing. The safe domain for the material is therefore assumed to be:

$$\sigma_t > \sigma > \sigma_c \quad \text{or} \quad \varepsilon_t > \varepsilon > \varepsilon_c \qquad (1)$$

where σ_t is the tensile strength, ε_t the critical strain in tension, σ_c the compression strength, ε_t the critical strain in compression and σ/ε the stress/strain in a material element. Note that according to the classical sign convention, tension is marked as positive and compression is marked as negative. This maximum stress/strain criterion is actually still widely used despite serious shortcomings. In the individual parts of an industrial refractory structure, operating loads generate complex and varying states of stresses. Combinations of tensile stresses in one direction, compression stresses in another or multiaxial compression and probably additional shear stresses are not unusual and likely to lead to failure of a refractory structure well below its tensile or compression strengths. In that respect, more complex failure criteria have been developed over the years. Most of them can be depicted as a surface called failure surface in the stress or strain space. Each point in the stress or strain space represents a combination of stresses/strains, i.e. a state of stress/strains. As long as the combination of stresses/strains under consideration lies below the failure surface (starting from an unloaded state), the material should remain intact. As soon as the failure surface is met or exceeded, a failure is expected to occur. Depending on the type of material considered, this surface takes different forms and the underlying functions are more or less complex.

The Drucker-Prager (D–P) failure criterion

Initially developed to deal with the plastic deformation of soils, the Drucker-Prager failure criterion proposed a rather simple approach to describe the behaviour of pressure dependant materials and was successfully applied to assess the failure threshold of rocks, concretes, polymers and foams. The D–P failure surface takes the form of a cone with its symmetry axis corresponding to the "identity line" (x = y = z line) in the stress space (Fig. 1). This conical surface can be simplified to a line with a smart change of coordinate system, the D–P failure line in the p–q space (Fig. 2):

$$p = -\frac{1}{3}(\sigma_x + \sigma_y + \sigma_z)$$

hydrostatic (or mean) stress (2)

$$q = \sqrt{\sigma_x^2 + \sigma_y^2 + \sigma_z^2 - \sigma_x \cdot \sigma_y - \sigma_x \cdot \sigma_z - \sigma_y \cdot \sigma_z + 3\left(\tau_{xy}^2 + \tau_{xz}^2 + \tau_{yz}^2\right)}$$

von Mises stress (3)

where, σ_x is the stress in the x-direction, τ_{xy} the shear stress in the xy-plane, σ_y the stress in the y-direction, τ_{xz} the shear stress in the xz-plane, σ_z the stress in the z-direction, τ_{yz} the shear stress in the yz-plane

$p = q \cdot tan(\varphi) + c$, equation of the D–P failure line in the p–q space (4)

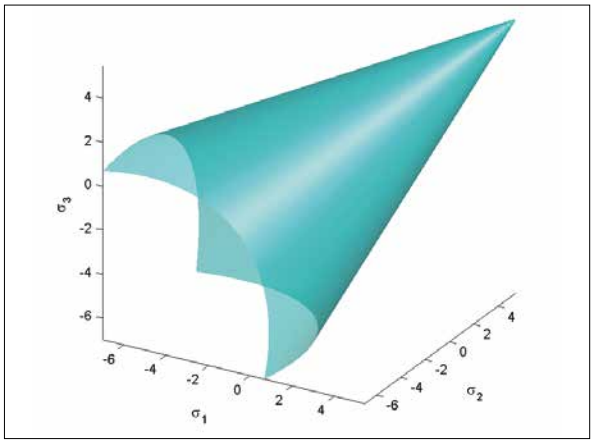

Fig. 1 Graphical representation of the Drucker-Prager failure surface in the stress space (principal stresses, source: Wikipedia)

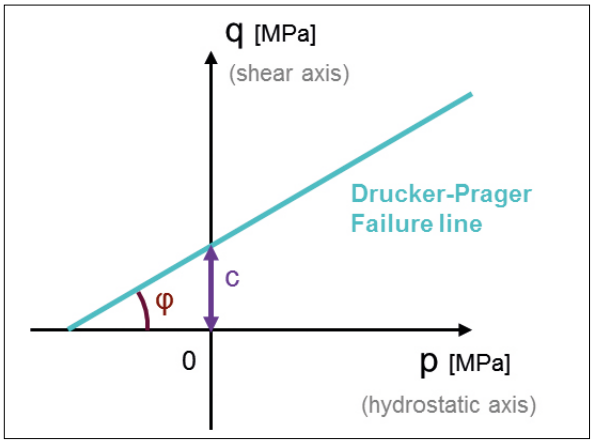

Fig. 2 Graphical representation of the Drucker-Prager failure line in the p–q space

where *c* is the intercept of the failure line with the q axis and *tan (ϕ)* is the slope of the failure line. The quantity *c* is usually called the cohesion and corresponds to the force due to intergranular bonds which tend to hold a coarse grained material together. The angle *ϕ* is called the angle of friction and corresponds to the resistance to shear stresses due to friction and interlocking of the grains.

The D–P failure line describes the failure threshold for a material under all possible configurations of stresses. In practical terms, it needs two points to define a line. That means in the case of the D–P failure line, the results from mechanical testing under two different configurations of stresses are necessary. The first and quite evident one for refractory materials is the measurement of compressive strength or crushing strength using uniaxial compression tests. A second one could be the tensile strength, which is actually very difficult to measure at room temperature, and even more so at high temperature. To cope with this issue, the diametral compression test was selected as the second point, namely a configuration of stresses, to calculate the D–P failure line for refractory materials up to high temperature. More details concerning the assessment of the D–P failure line can be found elsewhere [3].

2 Experimental procedure

2.1 Material

The preparation and the development of the high alumina refractory model castables considered for the simulation have been described elsewhere [4]. However, as a matter of practicability, a brief description of these model castables is set forth hereafter.

Two formulations, given in the Tab. 1, were selected for the present work. Both formulations were self-flowing calcium aluminate bonded high alumina castables (Al_2O_3 > 98 mass-%) with 5 % calcium aluminate cement (CAC) as binder. The first formulation (REF) contained the rather typical splintered tabular alumina with a moderately elongated shape and served as a reference, while in the second formulation the coarse grain fractions 1–6 mm were replaced by more compact rather cubic-shaped tabular alumina.

2.2 Steel ladle model

The steel ladle was selected as typical and characteristic high temperature vessel for the steel production in order to develop an exemplary numerical model to simulate the first heating of a refractory monolithic lining. Typically, steel ladles are composed of a steel shell, usually presenting a vertical tapered cone shape, with a mechanical lifting system for the transport, and a refractory lining inside to protect the steel shell and the environment from the high temperatures. The refractory lining itself commonly consists of at least two layers: the wear lining in contact with the molten steel and progressively "consumed" during the use of the ladle and the permanent (safety) lining, besides an additional isolation layer that is usually added between the permanent lining and the steel shell.

For the FEM simulation, the commercial software COMSOL Multiphysics was used. The first step to model the system was the definition of a simplified geometry. The shape and the dimension of the modelled steel ladle have been derived from a technical drawing. For the sake of simplification, the mechanical lifting system and other metallic protuberances were ignored for

Tab. 1 Composition of the model castables [mass-%]

Castable	REF	C1-6
Tabular alumina (splintered)		
3,0 – 6,0 mm	16	0
1,0 – 3,0 mm	21	0
0 –1 mm	41	41
Tabular alumina (cubic)		
3,0 – 6,0 mm	0	16
1,0 – 3,0 mm	0	21
Calcined alumina	10	10
Reactive alumina	7	7
CA cement	5	5
Dispersing agent (PCE)	0,15	0,15
Water	4,5	4,5

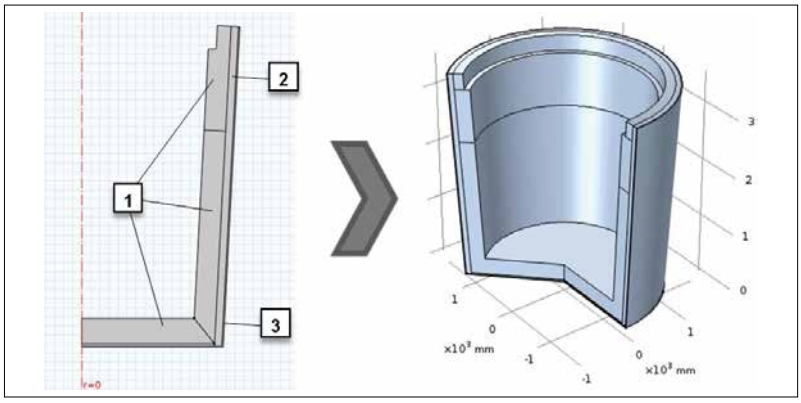

Fig. 3 2D-model of a steel ladle; 1: wear linings, 2: permanent lining, 3: steel shell

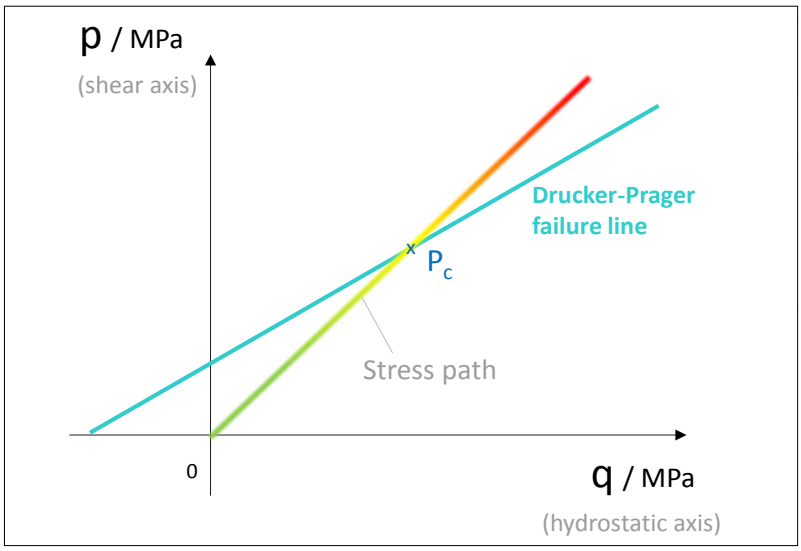

Fig. 4 Graphical representation of the tendency for failure for test piece being loaded under conditions of constant stress ratio and initially free of stress in the p–q space: green = low risk of failure, yellow = significant risk of failure, red = very high risk of failure

the simulation. On this basis and thanks to its tapered cone shape, the simplified ladle displays a vertical rotation axis, and a 3D-model was created from a rotationally symmetric 2D-geometry (Fig. 3).

The second step was to specify the material information and accordingly to define how the materials should behave. The steel for the shell was taken from the material library of COMSOL Multiphysics. For the refractory materials used in the linings, temperature-dependent material properties were either extracted from data sheets (cement bonded bauxite castable for the permanent lining) or obtained from own material investigations (model castables described in the Tab. 1).

As next step, the physics and multiphysics were selected. In the present case, the heat transfer (in solids) module and solid mechanics module were used. This led automatically to the use of the multiphysics thermal expansion. The different simulation conditions, such as initial values, axial symmetry, thermal isolation, heat flux, fixed and floating bearings, properties of the interface between materials, were then defined. In parallel, new formulas for the calculation of the D–P failure criterion were implemented. These new formulas were based on the stress path concept.

The stress path is used to represent the successive states of stress in a test piece during mechanical investigations. For most of the standard test procedures for refractory products, such as uniaxial compression test or three points bending test, a constant stress ratio ($\sigma_x = a \cdot \sigma_y = b \cdot \sigma_z$, where e.g. a = b = 0 for a uniaxial compression test in the x-direction) is applied to the test pieces initially free from external constraints ($\sigma_x = \sigma_y = \sigma_z = 0$). In this specific case the stress path follows a straight line from the origin ($\sigma_x = \sigma_y = \sigma_z = 0$) until the point of failure (σ_c) in the stress space. In the p–q space, loading under conditions of constant stress ratio also follows a straight line from the origin (p = q = 0) until the point of failure (P_c). It is worth noting that the point of failure P_c for a given constant stress ratio corresponds to the intersection between the stress path (and its prolongation) and the D–P failure line (Fig. 4).

Since practically real test pieces, especially refractory products, do not fail at a perfectly defined loading value, i.e. a more or less widespread distribution of strengths is measured, only a risk of failure or a tendency for failure can be assessed. The closer a point P on the stress path is to the D–P failure line (but still below the failure line), the higher the test piece is at risk of failing. Conversely, and obviously, the closer to the origin a point P is located (i.e. low level of stresses), the safer is the test piece (low risk of failing). Finally, and likewise, the further away is the point P on the prolongation of stress path away from the D–P failure, the higher is the probability that the test piece already has failed. In mathematical terms, this tendency for failure R at a point $P(\sigma_x, \sigma_y, \sigma_z, \tau_{xy}, \tau_{xz}, \tau_{yz})$ can be expressed, in the p–q space, as the ratio of the distance Dp between the origin and the point $P(p_p, q_p)$ to the distance D_{Pc} between the origin and the point $P_c(p_{Pc}, q_{Pc})$.

$$R = \frac{D_P}{D_{Pc}} \qquad (5)$$

where $D_p = \sqrt{p_p^2 + q_p^2}$ and

$$Dp = \sqrt{p_{Pc}^2 + q_{Pc}^2}$$

If $R \cong 1$, significant risk of failure
$R << 1$, low risk of failure
$R >> 1$, very high risk of failure.

Knowing the state of stress at the point P, p_p and p_q can be calculated using the eq. (2) and (3).

As previously mentioned, the point $P_c(p_p, p_q)$ corresponds to the intersection between the Drucker-Prager failure line $p = q \cdot tan(\phi) + c$ and the stress path $p = q \cdot (p_p/p_q)$. Accord-

ingly, the coordinates (p_{pc}, p_{qc}) of the point P_c are obtained by solving the following system of two equations with two unknowns:

$$\begin{cases} p_{P_c} = q_{P_c} \cdot tan(\varphi) + c \\ p_{P_c} = q_{P_c} \cdot (q_P / p_P) \end{cases} \quad (6)$$

then,

$$\begin{cases} p_{P_c} = \dfrac{c}{q_P/p_P - tan(\varphi)} \\ q_{P_c} = \dfrac{c}{1 - p_P/q_P \cdot tan(\varphi)} \end{cases} \quad (7)$$

Combining the equations (2), (3), (5) and (7), it is therefore possible to calculate a tendency for failure R at any stage of testing for a test piece being loaded under conditions of constant stress ratio and initially free of stress.

In most practical applications, however, each location of the system under consideration, for instance of a refractory lining of furnaces and process units, experiences different states of stress and follows its own, more or less complex, stress path. Thanks to the numerical simulation, the state of stress at each point of the modelled system can be assessed. From the state of stress at a given location of the model, the position of its point in the p–q space can be calculated (equations (2) and (3)), and more specially, if this this point lies below (= "safe") or above (= "failed") the D–P failure line worked out. This leads to binary outcomes, i.e. "safe" or "failed".

In order to assess the risk of failure in complex systems, the following assumptions and simplifications were made: at any time and at any location (element) of the modelled system (i.e. refractory lining being heated up), the state of stress was considered as if this element, initially free of stress, would be loaded under conditions of constant stress ratio. At least during the first heating of a lining made from refractory castables, the stress paths in relevant positions of the refractory wear lining should not diverge excessively from a straight line in the p–q space. Therefore, by implementing the equations (2), (3), (5) and (7) to the state of stress assessed by the numerical simulation at each point of the model, it is anew possible to appraise a risk of failure during the first heat up. A distribution of risk is hence obtained, where values near to $R = 0$, displayed as green in the simulation results, indicate low risk of failure, and values near to $R = 1$ and above $R > 1$, displayed as yellow to red, indicate an increased risk of failure or guarantee failure ($R >> 1$).

Tab. 2 D–P parameters for the formulation REF and C1–6 with increasing temperature

Temperature	REF		C1-6	
	c [MPa]	Φ [°]	c [MPa]	Φ [°]
Room temperature	14,2	65,9	14,8	66,7
450 °C	21,7	64,5	14,1	68,6
700 °C	14,1	66,8	10,4	69,8
1000 °C	13,0	68,0	10,9	69,1
1250 °C	18,6	66,1	14,6	67,8
1450 °C	–	–	29,1	58,5
1500 °C	25,2	61,2	–	–

3 Results and discussion

3.1 Assessment of the D–P failure lines

The equation of D–P failure lines, or more especially the cohesion c and angle of friction ϕ, were assessed for the formulation REF and C1–6 (Tab. 1) from uniaxial and diametral compression measurements at different temperatures (more details in [3]). The D–P parameters c and ϕ are given in the Tab. 2.

The differences in cohesion c and angle of friction ϕ between the two formulations are not self-explanatory. One might have expected that interlocking effects, from the more elongated and angular splintered grains in formulation REF, lead to higher values of angles of internal friction. Actually, the opposite was observed. The greater ability of cubic grains in formulation C1–6 to be piled up, and thus to form a compact skeleton of coarse grains, was thus thought to account for the increase of the angle of internal friction compared to formulation REF. Beyond that, the effect of the temperature was found to be quite forthright, with sintering as well as the growth of hibonite promoting an increase of the cohesion at high temperature. On the other hand, the formation of the first and very low amount of liquid phases at the grain boundaries might cause the observed decrease of the angle of internal friction at high temperature.

3.2 Modelled steel ladle

Because of the casting process for the monolithic linings, the thermal contact resistance between the two refractory linings (wear and permanent linings) as well as between the refractory permanent lining and the steel shell, was assumed to be negligible (good contact). That means that at the interface between the refractory wear and permanent linings, as well as between the refractory permanent lining and the steel shell, the temperature of both materials is taken as identical and the flow of heat is uniform over the whole contact surface. At the interface between the steel ladle and the surrounding environment, a mild heat transfer (h = 20 W · m^{-2} · K^{-1}) was considered. This corresponds to the expected heat transfer coefficient for gases (surrounding atmosphere) in contact with solids and in free convection (convective heat transfer).

One of the main challenges was to simulate the heat up process of the refractory lining in a simple and effective manner. To achieve this, a single heating curve was used in combination with changes of the heat transfer coefficient to differentiate between the pre-heating process with gas burner and the filling with the hot molten metal. Practically, in order to avoid massive thermal spalling or even the explosion of the monolithic lining due to the arising of high pressure steam, a carefully controlled heat up program is being observed (Tab. 3). Up to almost 1300 °C, the lining is pre-heated with gas burners and the heat transfer coefficient set to 150 W · m^{-2} · K^{-1}, which is approximately the expected value for refractory products heated by a gas burner. After 64 h pre-heating, the filling of the steel ladle with molten metal (tapping) is simulated by a sudden increase of the temperature at the hot face as well as strong increase of the heat transfer coefficient, since the contact with hot molten metal promotes a much more efficient heat transfer compared to a flame from a gas burner.

Tab. 3 Heating program and heat transfer coefficient applied at the hot face of the wear lining

Start [h]	End [h]	Temperature Function [°C]	Heat Transfer Coefficient [W · m^{-2} · K^{-1}]
0	6,5	20 · t + 20	150
6,5	37,75	8 · t + 98	150
37,75	49	30 · t – 730	150
49	64	40 · t – 1215	150
64	70	1700	1500

Once again, because of the casting process and nature of the monolithic linings, the bond between the wear and permanent linings was assumed to be almost as strong as the bond in the linings bulk. This means that the strains and stresses were completely transmitted at the contact interface between wear and permanent linings. In contrast, the bond between the permanent lining and the metal shell was assumed to be weak. To simulate this, a virtual thin layer at the interface permanent lining to the metal shell was implemented. This layer displays elastic properties and its spring constant set as low as possible (10 N · m^{-1} · m^{-2}).

Since the direct comparison of the arising stresses would be very tricky, the following discussions focus on the implementation of the failure criterion in the simulation. It should be noted that, since the materials properties other than the mechanical properties did not vary and/or were not expected to vary significantly between the two model castable formulations REF and C1–6, the only difference in the simulation between

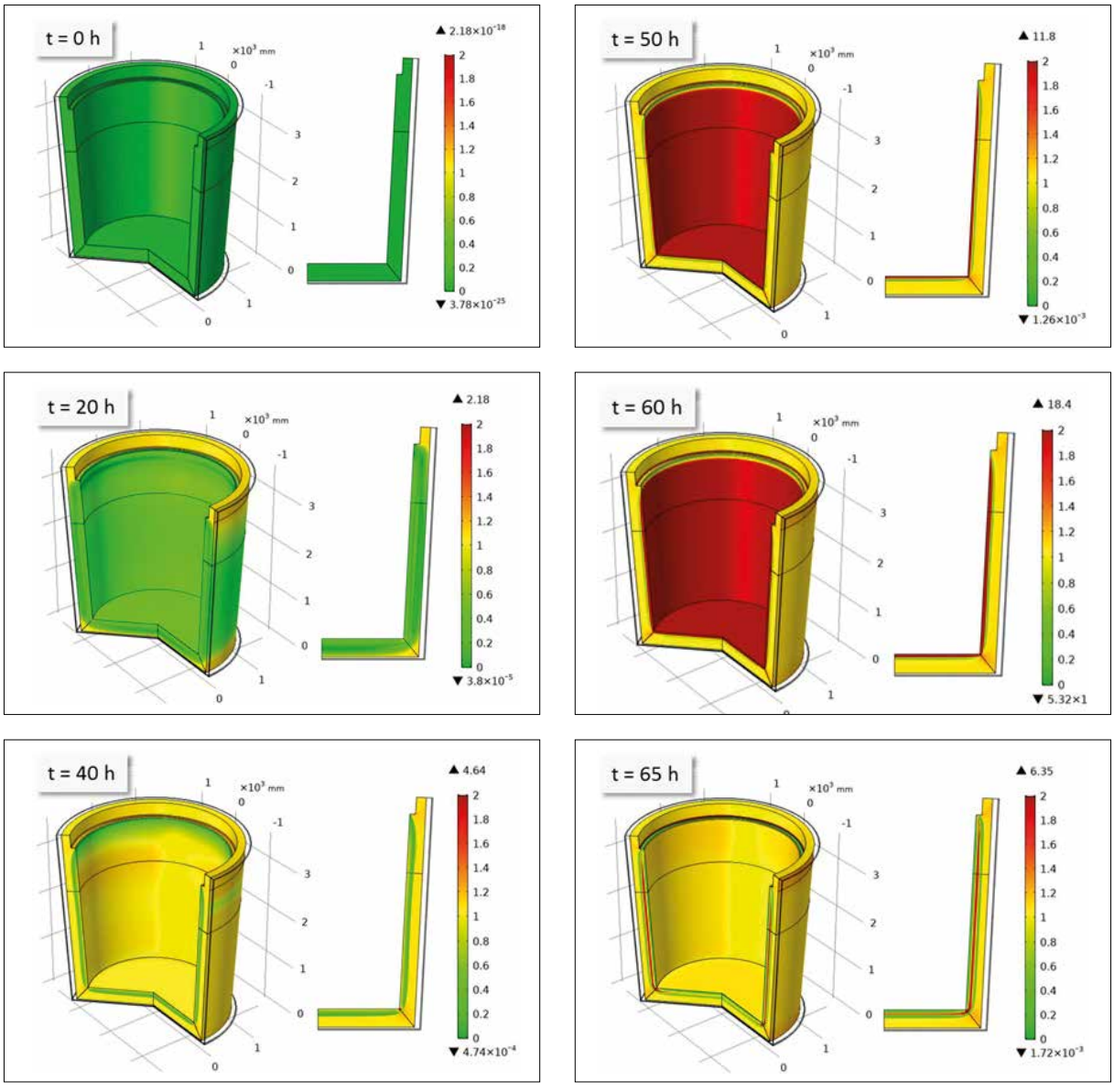

Fig. 5 Evolution of the risk of failure R during the simulated pre-heating (0–64 h), and filled with molten metal (after 64 h) – wear lining made of the MCA REF

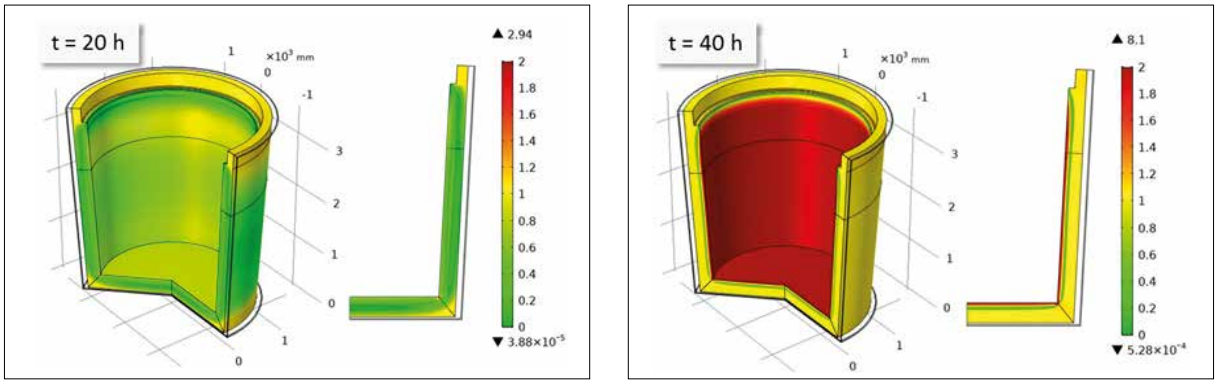

Fig. 6 Risk of failure R after 20 h and 40 h of pre-heating – wear lining made of MCA C1–6

the two castables lies above all in the values for the D–P parameters cohesion and angle of friction ϕ. Consequently, the simulated temperatures and stress distributions are almost identical for the two castable formulations and this permits a direct comparison and investigation of the influence of the D–P parameters.

Starting from a state of zero stress and accordingly no risk of failure, the likelihood that a lining is being damaged increased rapidly as the temperature at the hot face increased. Severe local stress concentration, and accordingly high value of R, arose very soon during preheating at corners and

edges of the refractory lining (Fig. 5). Indeed, these areas are known to be prone to spalling or crack initiation. Between 40–64 h of heat up (pre-heating), the whole hot face became at high risk of failure, actually it is quite common to observe the formation cracks at this stage of the heat up, or even sooner.

It is also worth noting that there exists a zone at low risk of failure in middle of the thickness of a lining. This corresponds to the neutral fibre of the system, where basically the transition from compressive stresses at the hot face to tensile stresses in the colder parts occurs. 1 h after the filling with molten metal (i.e. at 65 h of the simulation), the risk of failure at and immediately near the hot face decreased significantly. Two main factors could be behind this evolution: on the one hand, as the temperature at the hot face did not raise anymore (molten metal was considered to have a constant temperature), the thermal gradient flattened with time and stresses decreased. On the other hand, the cohesion of material increased at high temperature, which seems to promote the resistance to failure.

When comparing the evolution of *R* between the two model castable formulations, a similar behaviour is observed but overall the risk of failure is found to be significantly higher in castable formulations containing cubic tabular alumina (TA) C1–6 (Fig. 6). With regard to the simulation, the main difference between the castable formulation that contained only splintered TA (REF) and those containing cubic TA (C1–6), is the lower angle of friction and higher cohesion values for the reference formulation containing only splintered TA as can be seen in the Tab. 2. Since, despite overall lower angle of friction, the castable formulation that contained only splintered TA (REF) seemed to perform better, the cohesion appeared to be the key to optimize the failure tendency of refractory castables.

4 Conclusions

Refractory materials, as most ceramic materials, display great compression capability, however they are much more sensitive to tensile loads. Additionally, the stress distributions arising in industrial refractory structures like refractory linings are far more complicated than the stress distributions induced by classical laboratory tests. Accordingly, to be able to predict the failure of industrial refractory structures under operating conditions, a method to determine a more practice oriented failure criterion was set up and implemented into a simulation to assess the tendency for failure of the wear lining of a steel ladle. To this end a new algorithm, based on the Drucker-Prager (D–P) criterion, was developed. It allows not only to identify whether or not a part of the lining may fail, but also to provide a distribution of risk of failure for a lining during the heat up process. The risk of failure was quantified with a dimensionless parameter *R*. First results using the D–P failure parameters showed that the likelihood that the lining becomes damaged increased rapidly as the temperature at the hot face increases. Severe concentrations of local stress, and accordingly high value of R, arise very soon at corners and edges of refractory linings. Indeed, these are known to be prone to spalling or crack initiation. At least after 40 h of pre-heating, the whole hot face became at high risk of failure, actually it is not usual to observe the formation of cracks at this stage of the heating up, or even sooner. 1 h after the filling with molten metal, the risk at and immediately near to the hot face of a lining dropped significantly.

When comparing the evolution of *R* between tow model cement bonded castable formulations, a similar simulated behaviour is observed but the overall risk of failure is significantly higher in castable formulations containing cubic Tabular Alumina (TA). Since, despite overall lower angle of friction, the castable formulation that contained only splintered TA seemed to perform better, the cohesion appeared to be the key to optimize the failure tendency of refractory castable. The development of formulations with grains presenting even more angular and/or elongated shapes than the splintered TA to enhance the cohesion, could therefore be a way to significantly improve the performance of refractory castables, and potentially even shaped refractory products.

Acknowledgements

The authors would like to thank the German Federation of Industrial Research Associations (AiF) for its financial support of the research project IGF-No. 174 EN. This project was implemented under the CORNET initiative and carried out under the auspices of AiF and financed within the budget of the Federal Ministry for Economic Affairs and Energy (BMWi) through the programme to promote collective industrial research (IGF), as well as within the budget of the Public Service of Wallonia (SPW).

References

[1] Chapra, S.C.; Canale, R.P.: Numerical Methods for Engineers, 2nd Ed., McGraw-Hill Book Company, 1988

[2] Timoshenko, S.; Goodier, J.N.: Theory of elasticity, 3rd Ed., McGraw-Hill, New York, USA, 1987

[3] Brochen, E.; Dannert, Chr.; Erbar, L.; Krause, O.; Abdelouhab, S.: Tailoring the shape of coarse grains in castables – Investigation of the failure tendency of refractory castables during the first heating, implementation of an improved failure criterion. Materiały Ceramiczne/Cerami. Mat., in press

[4] Erbar, L.; Krause, O.; Brochen, E.; Dannert, Chr., Abdelouhab, S.: Impact of cubic-shaped grain fractions on the working properties and green strength of high-alumina castables. Proceedings of the 61st International Conference on Refractories, Aachen, 2018